HNPS Advances in Nuclear Physics

Vol 23 (2015)

HNPS2015

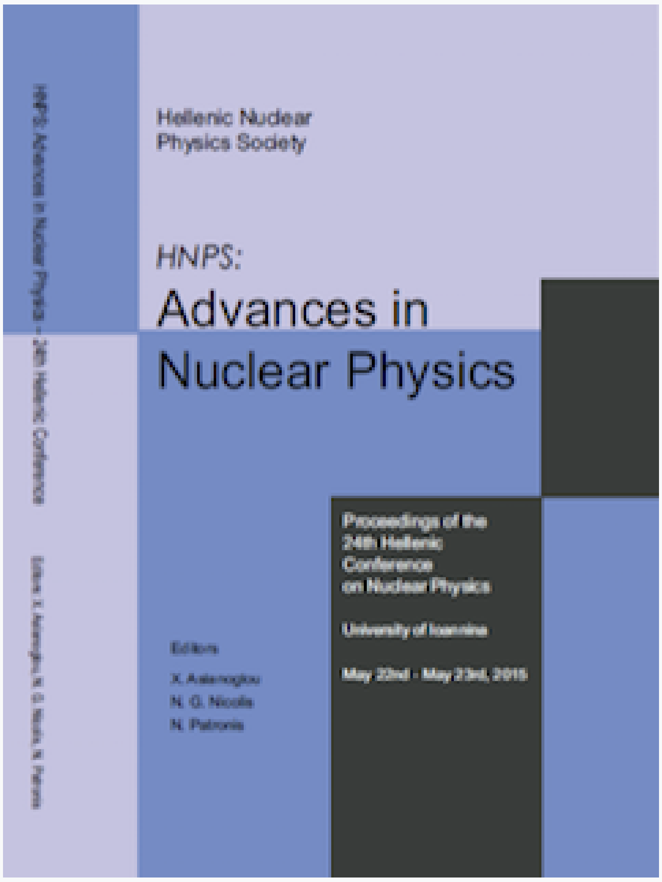

Prediction of high-K isomeric states in transactinide nuclei close to N=162

V. Prassa, B.-N. Lu, T. Niksic, D. Ackermann, D. Vretenar

doi: [10.12681/hnps.1909](https://doi.org/10.12681/hnps.1909)

Prediction of high-K isomeric states in transactinide nuclei close to N=162

V.Prassa[1,*], Bing-Nan Lu[2], T. Niksic[1], D. Ackermann[3], D. Vretenar[1]

[1] *Physics Department, Faculty of science, University of Zagreb, 10000 Zagreb, Croatia*
[2] *Institut fur Kernphysik, Institute for Advanced Simulation, and Julich Center for Hadron Physics, Forschungszentrum Julich, D-52425 Julich, Germany*
[3] *GSI Helmholtzzentrum fur Schwerionenforschung GmbH, Planckstrasse 1, 64291 Darmstadt, Germany*

Abstract Transactinide nuclei around neutron number N=162 display axially deformed equilibrium shapes. In the present study we are particularly interested in the occurrence of high-K isomers in the axially deformed isotopes of Rf (Z=104), Sg (Z=106), Hs (Z=108), and Ds (Z=110), with neutron number N=160-166 and the effect of the N=162 closure on the structure and distribution of two-quasiparticle (2qp) states. The evolution of high-K isomers is analyzed in a self-consistent axially symmetric relativistic Hartree-Bogoliubov calculation using the blocking approximation with time-reversal symmetry breaking.

Keywords high-K isomers, transactinides, nuclear density-functionals

---

INTRODUCTION

Nuclei beyond the actinides owe their existence to the underlying single-nucleon shell structure. These elements often display axially deformed equilibrium shapes and intruder single-nucleon states with high-Ω values (projection of the single-particle angular momentum onto the symmetry axis of the nucleus) appear close to the Fermi level. The unpaired quasiparticle excitations form isomeric states with high values of total $K = \Sigma_i \Omega_i$ [1]. Because they can only decay by K-forbidden transitions, these states have lifetimes that are significantly longer than most of the neighboring states. The decay of isomeric states provides information on the nuclear wave function, single-nucleon states, pairing gaps and residual interactions [2].
Systematic experimental efforts in the region of very heavy nuclei have produced detailed spectroscopic data in nuclei around ^{254}No [3- 7]. In addition to the detection of α and γ decays, recent studies have made use of conversion electrons (CE) to investigate possible K-isomeric states in heavy high-Z nuclei such as, for instance, ^{256}Rf, in which internal conversion becomes the preferred decay mode [8, 9]. The heaviest nuclei for which characteristic high-K isomeric decays have been investigated are ^{270}Ds and its α-decay daughter ^{266}Hs [10, 11]. Theoretical studies of quasiparticle excitations in the region of transactinide nuclei have been based on the microscopic-macroscopic approach [12-23], self-consistent models with Skyrme functionals [24-29], the Gogny force [30-32], and relativistic energy density functionals [33-38].

---

* Corresponding author, email: vprassa@gmail.com

In the present study [39] we extend our resent study of shape evolution, collective excitation spectra, and decay properties of transactinide nuclei based on the microscopic framework of relativistic energy density functionals Ref. [33], to two-quasiparticle excitations in the axially deformed isotopes of Rf (Z = 104), Sg (Z = 106), Hs (Z = 108), and Ds (Z = 110), with neutron number N = 160 − 166.

QUASI-PARTICLE EXCITATIONS

The two-quasiparticle neutron or proton states are obtained in a self-consistent relativistic Hartree-Bogoliubov calculation [39, 40], based on the functional DD-PC1 [41] and with a separable pairing force of finite range [42, 43], using the blocking approximation with time-reversal symmetry breaking. The 2*qp* states are determined by blocking the lowest neutron or proton quasi-particle orbitals located in the vicinity of the Fermi energy that corresponds to the fully paired equilibrium solution. After performing the iterative minimization, the energy of the two-quasiparticle excitation is obtained as the difference between the energy of the self-consistent blocked RHB solution and the energy of the fully paired equilibrium minimum. The breaking of time-reversal symmetry removes the degeneracy between signature partner states with angular-momentum projection on the symmetry axis $K_{\mathrm{min}} = |\Omega_i - \Omega_j|$ and $K_{\mathrm{max}} = \Omega_i + \Omega_j$, and with parity $\pi = \pi_i \cdot \pi_j$.

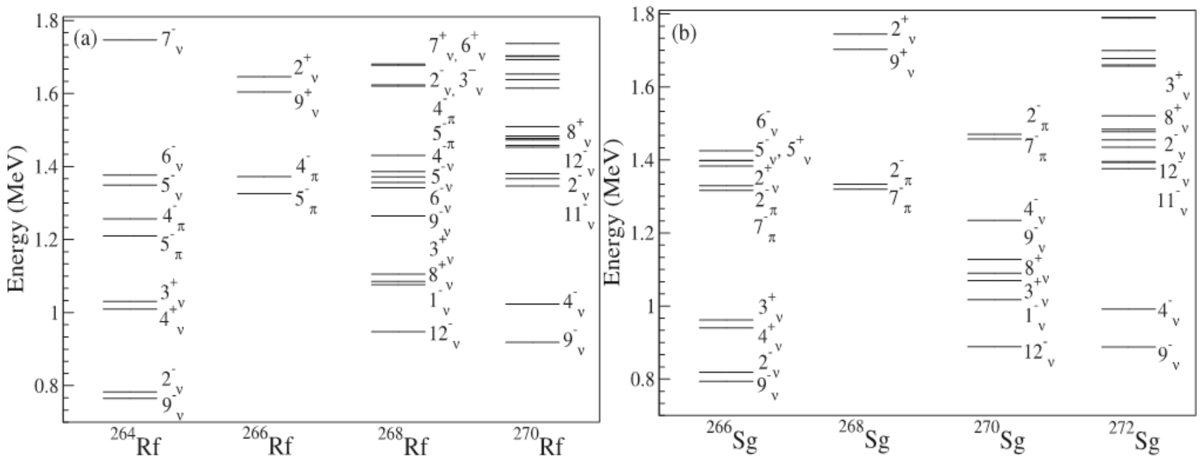

Fig. 1.Lowest two-quasiparticle states in Rf (upper panel) and Sg (lower panel) isotopes with neutron number N = 160 − 166. The 2*qp* states correspond to axially symmetric solutions obtained with the relativistic functional DD-PC1 and a pairing force separable in momentum space. The calculation includes time-reversal symmetry breaking.

Figures 1 and 2 display the excitation energies of two-quasiparticle $K_{\nu(\pi)}$ states for the Rf, Sg, Hs and Ds isotopes with neutron number N = 160 − 166. In figure 1 the high density of single-particle levels close to the Fermi surface in the isotopes of Rf and Sg with N=160 yields a number of quasiparticle excitations in the energy window below 1.8 MeV. Our calculation predicts the occurrence of the two-neutron isomeric states $K^{\pi} = 9^{-}_{\nu}$ and 2^{-}_{ν}

originating from the single-particle orbitals $\nu 7/2^+[613] \otimes \nu 11/2^-[725]$. The neutron orbitals $\nu 1/2^+[620]$ and $\nu 7/2^+[613]$ are coupled to form the states 4^+_ν and 3^+_ν at excitation energy close to 1MeV. An interesting result, that can also be noticed in the two other isotopic chains considered in this study, is that the lowest two-quasiparticle states in the *N* = 162 isotones are predicted at considerably higher excitation energies. For the particular choice of the energy density functional and pairing interaction used in this and our previous study [33], the lowest two-quasiparticle states typically occur at ≈ 0.8 MeV, whereas in the *N* = 162 isotones the excitation energies of the lowest 2*qp* states are predicted at E ≥ 1.2 MeV. For ^{266}Rf, in particular, the doublet of states 5^-_π and 4^-_π states at energy 1.35 MeV originates from the two-proton configuration $\pi 1/2^-[521] \otimes \pi 9/2^+[624]$. The lowest two neutron excitations occur at even higher energies: the 9^+_ν and 2^+_ν states at 1.60 MeV and 1.65 MeV, respectively, based on the high-j configuration $\nu 7/2^+[613] \otimes \nu 11/2^+[606]$. In ^{268}Sg, as a result of the neutron shell-closure at *N* = 162, the lowest 2*qp* excitations are the proton states 7^-_π and 2^-_π at 1.32 and 1.33 MeV, respectively, originating from the Nilsson levels $\pi 5/2^-[512]$ and $\pi 9/2^+[624]$. We note that for this nucleus the only two-neutron *qp* states, predicted below 1.8MeV are the 9^+_ν and 2^+_ν ($\nu 11/2^+[606] \otimes \nu 7/2^+[613]$) at 1.70 and 1.74 MeV, respectively. The occurrence of 2*qp* excitations in ^{268}Rf and ^{270}Sg already at energies ≈ 1 MeV is consistent with the increase of the single-particle level density near the Fermi surface. The lowest-lying two-neutron excitations 12^-_ν and 1^-_ν originate from the configuration $\nu 13/2^-[716] \otimes \nu 11/2^+[606]$. In ^{270}Rf and ^{272}Sg the lowest 2*qp* configurations are: $\nu 5/2^+[613] \otimes \nu 13/2^-[716]$ (9^-_ν and 4^-_ν), $\nu 9/2^+[604] \otimes \nu 13/2^-[716]$ (11^-_ν and 2^-_ν), $\nu 11/2^+[606] \otimes \nu 13/2^-[716]$ (12^-_ν and 1^-_ν), and $\nu 5/2^+[613] \otimes \nu 11/2^+[606]$ (8^+_ν and 3^+_ν).

In ^{268}Hs (left panel of figure 2), the lowest-lying 2*qp* excitations are the signature partner levels 9^-_ν , 2^-_ν and 4^+_ν , 3^+_ν. The two configurations coincide in energy, with the aligned Ω-states at 0.86 MeV and the anti-aligned ones at 0.88 MeV. Adding two more protons (right panel of figure 2), the doublet 4^+_ν and 3^+_ν ($\nu 1/2^+[620] \otimes \nu 7/2^+[613]$) becomes the lowest 2*qp* excitation in the nucleus ^{270}Ds. The partner levels 9^-_ν and 2^-_ν, which are the lowest 2*qp* states in the *N* = 160 Rf, Sg and Hs isotopes, are calculated ≈ 200keV higher in energy. The prediction of a high-K two-neutron quasiparticle configuration at energy ≈ 1 MeV is in agreement with the experimental observation of a two-neutron high-K isomeric decay in ^{270}Ds [11]. In ^{270}Hs, because of the deformed shell closure, the neutron two-quasiparticle states 9^+_ν and 2^+_ν are predicted at energies 1.65 and 1.69 MeV, respectively. The lowest-lying 2*qp* states calculated for ^{270}Hs are the proton excitations 7^+_π and 2^+_π , with the structure of Nilsson orbitals $\pi 5/2^-[512] \otimes \pi 9/2^-[505]$. ^{270}Hs has been observed in the reaction ^{248}Cm (^{26}Mg, 4n), however, because of the low production cross section and consequently low number observed events (3), no detailed spectroscopic data are available except for α decay energies and decay times [44]. The calculation for ^{272}Ds predicts the proton two-quasiparticle states 10^{-}_{π} and1^{-}_{π} based on the configuration $\pi 9/2^{-}[505] \otimes \pi 11/2^{+}[615]$. Because of the *N* = 162 deformed shell gap the two-neutron doublets 9^{+}_{ν} , 2^{+}_{ν} and 5^{+}_{ν} , 6^{+}_{ν} , appears only at higher excitation energies (1.5 MeV). ^{272}Ds is the α-decay daughter of ^{276}Cn, which could be produced in a similar way as ^{270}Ds [11] via the reaction ^{207}Pb(^{70}Sn, 1n)^{276}Cn. An order of magnitude lower production cross section could be compensated by higher beam intensities at future linear accelerator facilities, e.g. the LINAG project presently under construction for SPIRAL2 [45], or the project for a high-intensity continuous wave machine at GSI [45]. Consistent with the results obtained for Rf and Sg isotopes, ^{272}Hs, ^{274}Hs, ^{274}Ds and ^{276}Ds exhibit an increased density of two-quasiparticle states at low excitation energies. The lowest Nilsson levels that form the 2*qp* configurations in the energy window below 1.8 MeV are the $13/2^{-}[716]$, $11/2^{+}[606]$, $5/2^{+}[613]$ and $3/2^{+}[611]$ for neutrons, and the orbitals $11/2^{+}[615]$, $9/2^{-}[505]$ and $5/2^{-}[512]$ for protons.

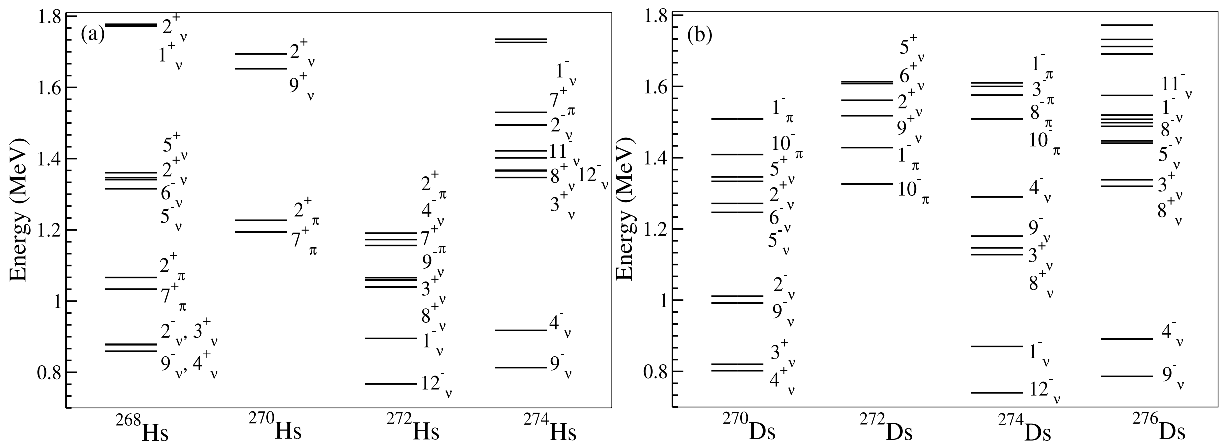

Fig. 2. Same as described in the caption to Fig. 1 but for the isotopes of Hs (upper panel) and Ds (lower panel).

CONCLUSIONS

In summary, we have employed the self-consistent mean-field framework based on relativistic energy density functionals to study the structure of two-quasiparticle excitations in axially deformed Rf, Sg, Hs, and Ds isotopes, with neutron number *N* = 160 − 166. The calculation of excitation energies of 2*qp* states is based on the blocking approximation with time-reversal symmetry breaking. Our microscopic self-consistent calculation has provided a detailed prediction for the evolution of 2*qp* states close to the *N* = 162 deformed-shell gap. The excitation energies of 2*qp* configurations depend on the specific choice of the energy density functional, and the strength of the pairing interaction. In the particle-hole channel we have used the relativistic functional DD-PC1 that was adjusted to the experimental masses of a set of 64 axially deformed nuclei in the mass regions $A \approx 150-180$ and $A \approx 230-250$. The strength of the separable pairing force of finite range was fine-tuned to reproduce the odd-even mass differences in the region $A \approx 230-250$. A stronger (weaker) pairing would automatically increase (decrease) the energies of the 2*qp* states (shown in Figs. 1 and 2) with respect to the corresponding ground states. The calculation predicts the occurrence of a series of low-energy high-K isomers, most notably the 9^{-}_{ν} in the N = 160 and N = 166 isotopes, and the 12^{-}_{ν} in the N = 164 nuclei. A very interesting result is the low density of 2*qp* states in the N = 162 isotones, with no two-neutron states predicted below 1.6 MeV excitation energy. The two-proton states in these nuclei are calculated almost 0.5 MeV higher in energy than the lowest 2*qp* states in neighboring isotopes. This is a consequence of the deformed-shell closure at N = 162 and presents an interesting observable that can be used, together with the separation energies and Q_{α}-values, to characterize the evolution of deformed shell gaps in this mass region, and possibly verified experimentally in the near future for ^{270}Hs and ^{272}Ds.

ACKNOWLEDGEMENTS
This work has been supported by the NEWFELPRO project of Ministry of Science, Croatia, co-financed through the Marie Curie FP7-PEOPLE-2011-COFUND program. Bing-Nan Lu and D. Vretenar acknowledge the support of the Helmholtz-Institut Mainz.

References

[1] K.E.G. Lo ¨bner, Phys. Lett. B 26, 369 (1968).
[2] P. M. Walker and G. D. Dracoulis, Nature 399, 35 (1999).
[3] R. -D. Herzberg and P. T. Greenlees, Prog. Part. Nucl. Phys. 61, 674 (2008).
[4] R. -D. Herzberg and D. M. Cox, Radiochim. Acta 99, 441 (2011).
[5] P. T. Greenlees et al., Phys. Rev. Lett. 109, 012501 (2012).
[6] B. Sulignano et al., Phys. Rev. C 86, 044318 (2012).
[7] J. Rissanen et al., Phys. Rev. C 88, 044313 (2013).
[8] H. B. Jeppesen et al., Phys. Rev. C 79, 031303(R) (2009).
[9] A. P. Robinson et al., Phys. Rev. C 83, 064311 (2011).
[10] S. Hofmann et al, Eur. Phys. J. A 10, 5 (2001).
[11] D. Ackermann et al., GSI Sci. Rep. 2011, 208 (2012); and to be published.
[12] S. Nilsson et al., Nuclear Physics A 115, 545 (1968).
[13] A. Sobiczewski, I. Muntian, and Z. Patyk Phys. Rev. C 63, 034306 (2001).
[14] A. Sobiczewski and K. Pomorski, Prog. Part. Nucl. Phys. 58, 292 (2007).
[15] A. Sobiczewski, Radiochim. Acta 99, 395 (2011).
[16] G. G. Adamian, N. V. Antonenko, and W. Scheid, Phys. Rev. C 81, 024320 (2010).
[17] A. N. Kuzmina, G. G. Adamian, and N. V. Antonenko, Phys. Rev. C 85, 027308 (2012).

[18] F. R. Xu, E. G. Zhao, R. Wyss, and P. M. Walker, Phys. Rev. Lett. 92, 252501 (2004).
[19] D. S. Delion, R. J. Liotta and R. Wyss, Phys. Rev. C 76, 044301 (2007).
[20] H. L. Liu, F. R. Xu, P. M. Walker, and C. A. Bertulani, Phys. Rev. C 83, 011303(R) (2011).
[21] H. L. Liu, F. R. Xu, and P. M. Walker, Phys. Rev. C 86, 011301 (2012).
[22] H. L. Liu and F. R. Xu, Phys. Rev. C 87, 067304 (2013).
[23] H. L. Liu, P. M. Walker, and F. R. Xu, Phys. Rev. C 89, 044304 (2014).
[24] S. Cwiok, J. Dobaczewski, P. H. Heenen, P. Magierski, and W. Nazarewicz, Nucl. Phys. A 611, 211(1996).
[25] S. Cwiok, W. Nazarewicz, and P.H. Heenen, Phys.Rev.Lett. 83, 1108(1999).
[26] T. Duguet, P. Bonche, and P.-H. Heenen, Nuclear Physics A 679, 427 (2001).
[27] M. Bender, P. Bonche, T. Duguet, and P.-H. Heenen, Nuclear Physics A 723, 354 (2003).
[28] M. Bender and P.-H. Heenen, J. Phys.: Conf. Ser. 420, 012002 (2013).
[29] Yue Shi, J. Dobaczewski, and P. T. Greenlees, Phys. Rev. C 89, 034309 (2014).
[30] J. L. Egido and L. M. Robledo, Phys. Rev. Lett. 85, 1198 (2000).
[31] J.-P. Delaroche, M. Girod, H. Goutte, and J. Libert, Nuclear Physics A 771, 103 (2006).
[32] M. Warda and J. L. Egido, Phys. Rev. C 86, 014322 (2012).
[33] V. Prassa, T. Niksic, and D. Vretenar, Phys. Rev. C 88, 044324 (2013).
[34] A. V. Afanasjev, T. L. Khoo, S. Frauendorf, G. A. Lalazissis, and I. Ahmad, Phys. Rev. C 67, 024309 (2003).
[35] V. Prassa, T. Niksic, G. A. Lalazissis, and D. Vretenar, Phys. Rev. C 86, 024317 (2012).
[36] E. Litvinova, Phys. Rev. C 85, 021303 (2012).
[37] A. V. Afanasjev and O. Abdurazakov, Phys. Rev. C 88, 014320 (2013).
[38] D. Vretenar, A. V. Afanasjev, G. Lalazissis, and P. Ring, Phys. Rep. 409, 101 (2005).
[39] V. Prassa, Bing-Nan Lu, T. Niksic, D. Ackermann, and D. Vretenar, Phys. Rev. C 91, 034324 (2015).
[40] J. Meng, H. Toki, S. G. Zhou, S. Q. Zhang, W. H. Long, and L. S. Geng, Prog. Part. Nucl. Phys. 57, 470 (2006)
[41] T. Niksic, D. Vretenar, and P. Ring, Phys. Rev. C 78, 034318 (2008).
[42] Y. Tian, Z. Y. Ma, and P. Ring, Phys. Lett. B 676, 44 (2009).
[43] T. Niksic, P. Ring, D. Vretenar, Y. Tian, and Z. Y. Ma, Phys. Rev. C 81, 054318 (2010).
[44] J. Dvorak et al., Phys. Rev. Lett. 97, 242501 (2006).
[45] R. Ferdinand, Proceedings of IPAC2014, Dresden, Germany, 1852 (2014).
[46] W. Barth, Proceedings of IPAC2014, Dresden, Germany, 3211 (2014).